Journal of Industrial and Engineering Chemistry xxx (2014) xxx–xxx

Contents lists available at ScienceDirect

Journal of Industrial and Engineering Chemistry

journal homepage: www.elsevier.com/locate/jiec

Pervaporation separation of butyric acid from aqueous and anaerobic digestion (AD) solutions using PEBA based composite membranes

Santosh K. Choudhari [a,b], Federico Cerrone [a,d], Trevor Woods [b,c], Kieran Joyce [e], Vincent O' Flaherty [a,f], Kevin O' Connor [a,d], Ramesh Babu [a,b,c,*]

[a] Technology Centre for Biorefining and Bioenergy, Ireland
[b] Center for Research on Adaptive Nanostructures and Nanodevices (CRANN), Trinity College, Dublin 2, Ireland
[c] School of Physics, Trinity College Dublin, Dublin 2, Ireland
[d] School of Biomolecular and Biomedical Sciences, UCD Conway and Institute and Earth Institute, University College Dublin, Ireland
[e] Centre for Microscopy and Analysis (CMA), Trinity College Dublin, Dublin 2, Ireland
[f] Microbiology Department, School of Natural Sciences and Environmental Change, National University of Ireland, Galway, Ireland

ARTICLE INFO

Article history:
Received 17 February 2014
Accepted 4 August 2014
Available online xxx

Keywords:
PEBA
Graphene
VFAs
Butyric acid
Pervaporation

ABSTRACT

Polyether block amides (PEBA) composite membranes were prepared by dispersing different two dimensional (2D) layered nanomaterials such as graphene, graphene oxide and molybdenum disulphide (MoS_2) in PEBA matrix. These composite membranes were applied for the pervaporation separation of butyric acid produced by anaerobic digestion (AD) of perennial grass. Among all the tested membranes PEBA–graphene membrane showed the best performance with butyric acid flux og 24.3 g/m^{2}h and separation factor of 21. Further on varying the graphene content in the membranes showed improved separation efficiency with increased thermal and mechanical properties of the membranes.

Introduction

Anaerobic digestion (AD) is a process in which a variety of different species from two entirely different biological kingdoms, bacteria and archaea, work together to convert organic wastes through a variety of intermediates into methane gas [1]. AD process is considered to be one of the most efficient waste and wastewater treatment technology. It offers number of significant advantages such as low sludge production, low energy requirement, high organic loading rates, and energy production in the form of methane. However, due to low calorific value and storage difficulties of methane, production of valuable fermentation intermediates such as volatile fatty acids (VFAs) have wider applications [2].

VFAs are short-chain fatty acids containing single carboxylic group such as formic, acetic, propionic and butyric acid. VFAs are valuable chemical products, especially butyric acid has diverse uses in the market. Butyric acid is employed in the diary or food industries to increase the fragrance of beverages or foodstuffs, and its potentials as pro-drug have raised an increasing interest in pharmaceutical industry [3,4]. Butyric acid is also used as raw material for the production of biodegradable polymers based on β-hydroxybutyrate [5]. More importantly it can be used as a precursor to produce butanol, ethyl butyrate and butyl butyrate, which have great potential to be used as fuels [6,7]. However, production of butyric acid via AD process is difficult due to its inhibitory effects on the process. Undissociated VFAs can freely permeate the cell membrane lowering pH within the cell [8]. Accumulation of certain VFAs may alter the anaerobic digestion process, causing reactions to became thermodynamically unfavourable, which may result in changes of the pathway of certain reactions [9]. Therefore, in order to prevent the inhibition, optimize the butyric acid production, and recover as valuable commodity chemicals, VFAs should be removed from the AD process.

Various techniques have been applied for the recovery of organic acids from aqueous solutions, including; electrodialysis [10,11], ion-exchange resin [12], adsorption [13], liquid–liquid extraction [14–16] and pervaporation [17,18]. Among these, pervaporation appears to be very promising. It is a membrane separation process based on the difference in solubility and

* Corresponding author at: School of Physics, Trinity College Dublin, Dublin 2, Ireland. Tel.: +353 18962602.
E-mail addresses: babup@tcd.ie, ramesh.padamati@gmail.com (R. Babu).

http://dx.doi.org/10.1016/j.jiec.2014.08.010
1226-086X/

diffusivity of the components to be separated through a dense membrane [19]. Pervaporation is very economical and environmentally friendly method compared to the other separation techniques and more importantly it has no harmful effects on the microorganisms and it can be directly coupled with anaerobic digestion chamber to continuously remove the inhibitory products.

With the rapid development of nanotechnology, the studies of mixed matrix composite membrane have attracted much attention in the last decade. The combination of individual properties of polymers and nano-size particle fillers creates synergistic characteristics for composite membranes, which makes them a group of promising materials for pervaporation separations. Common nanoparticles used in organic separations include zeolite [20–22], silica [23], carbonaceous particles [24,25] and show facilitating effects to enhance the pervaporation separation performance.

Recently, the unique physiochemical properties of two dimensional (2D) carbon and inorganic nanostructures such as graphene, graphene oxide and molybdenum disulfide 2D layered materials have been harnessed for a variety of potential applications, such as components in energy and semiconductor electronic devices, [26] dispersing agents for processing of liquid crystals,[27] porous scaffolds for tissue engineering,[28] and agents for bioimaging and drug delivery [29,30] and more importantly in the field of membrane separation application [31,32]. 2D based composite membranes showed some remarkable improvement in the separation ability [31,32].

To the best of our knowledge, this is the first report on use of PEBA membranes for separation butyric acid produced by AD process using pervaporation process. In view of this initially we tried to develop PEBA based composite membranes by dispersing different 2D nanostructured materials such as graphene, graphene oxide and molybdenum disulphide and applied them for the PV separation of butyric acid from AD solution. Based on preliminary PV results best filler was selected and further studied for effect filler loading, effect of feed temperature, effect of feed pH and effect of multiple component feed mixture. Butyric acid separation from AD solution was also studied and all the results were discussed in terms of PV separation efficiency of the membranes. To the best of our knowledge there is no report has been published comparing the effects of various layered nanomaterials on the PV performance of PEBA composite membranes.

Experimental

Materials

PEBA 2533 SA01 was obtained from Arkema (France). Graphene was procured from XG Sciences (USA). Graphene oxide was purchased from Cheapstubes.com (USA). Butanol, butyric acid, acetic acid, propionic acid valeric acid, Molybdenum (IV) sulphide, NaOH and H_2SO_4 were purchased from Sigma-Aldrich (Ireland). All the chemicals are of reagent grade and were used without further purification. Deionised water was used throughout the study.

Membrane preparation

Required amount of nanofiller was weighed and dispersed in 100 ml butanol. The solution was sonicated for 2 hours. To this a known amount of PEBA polymer was weighed and added to make 5 wt% solution. The polymer was dissolved by heating the solution at 80 °C under vigorous stirring for 24 h. Further the solution was cooled to room temperature and a definite amount of solution was poured into a glass petri dish and kept for drying at room temperature for 2 days. After that membranes were peeled off and further dried in vacuum oven at 50 °C for 24 h to remove the residual solvent in the membrane. Pure PEBA membrane was prepared in a similar way without adding any nanofiller.

Membrane characterisation

Contact angle of the membranes were measured through sessile drop method using in-home designed apparatus at 25 °C. Membranes were dried overnight in a vacuum oven at 50 °C prior to the contact angle measurements. A piece of membrane (1 cm × 5 cm) was adhered to clean and smooth glass slide on which 2 μL of deionized water droplet was placed and the droplet image was captured using a microscope coupled with a CCD camera. All the reported values are the averages of five measurements taken at different locations of the same membrane surface.

Tensile measurements were carried out using a Zwick twin column tensile tester with a 100 N load cell and calibrated with a 2 kg standard. The tensile tests were carried out at room temperature on rectangular samples with dimensions of (10 × 2) mm and a cross head speed of 25 mm/min. Young's modulus, ultimate tensile strength and elongation at break were calculated.

Differential Scanning Calorimetry (DSC) was performed with Perkin Elmer Pyris-Diamond Calorimeter. The samples weighing 7–8 mg were encapsulated in hermetically sealed aluminium pans and heated from −90 °C to 200 °C at a rate of 10 °C/min under nitrogen atmosphere. The Tm and ΔHm of the membranes were determined by using the thermograms obtained.

Thermal stability of the membranes were analysed through thermo gravimetric analysis (TGA) using Perkin Elmer Pyris 1 Thermo gravimetric Analyser in air atmosphere. The instrument was calibrated using nickel and iron standards and sample weighing ∼7 mg is placed in a platinum pan and heated from 30 °C to 700 °C at the heating rate of 10 °C/min.

Anaerobic digestion (AD) process

AD solution was produced following the procedure given in [33]. In brief, AD process was carried out in a specially designed leach bed reactor and whole-crop of perennial grass was used as substrate for anaerobic digestion. Three leach bed reactors were operated for 14 days each at 37 °C. To start the batch, all reactors were filled with ∼1.1 kg of a mix containing ∼280 g of granular sludge derived from a full scale reactor digesting dairy wastewater and ∼820 g of ensiled grass. This gave a volatile solid (VS) content of ∼200 g, of which ∼170 g was fresh substrate. After the reactors were filled with the solid mixture, 2 L of leachate solution was added to the control reactor and the same leachate containing sodium bicarbonate ($NaHCO_3$) was added to the experimental reactors. The sodium bicarbonate concentration was calculated to maintain pH at the desired range (5.0 or 6.0). The reactors were then sealed. The leachate was continuously recirculated from the bottom of the reactor to the top by a peristaltic pump. At the end of each AD leachate bed reactor batch, the leachates were drained, collected and stored at −20 °C. The anaerobic digestion of grass resulted in the production a VFA mixture composed of acetic acid, propionic acid, butyric acid and valeric acid of 0.52, 0.23, 5.95 and 0.60 g/L respectively and a total concentration of 7.3 g/L. All the samples were thawed overnight prior to use for the PV separation experiments.

Pervaporation experiments

Pervaporation experiments were carried out using indigenously designed pervaporation experimental set-up shown in Fig. 1. The membrane was mounted in a stainless steel permeation cell, with

Please cite this article in press as: S.K. Choudhari, et al., J. Ind. Eng. Chem. (2014), http://dx.doi.org/10.1016/j.jiec.2014.08.010

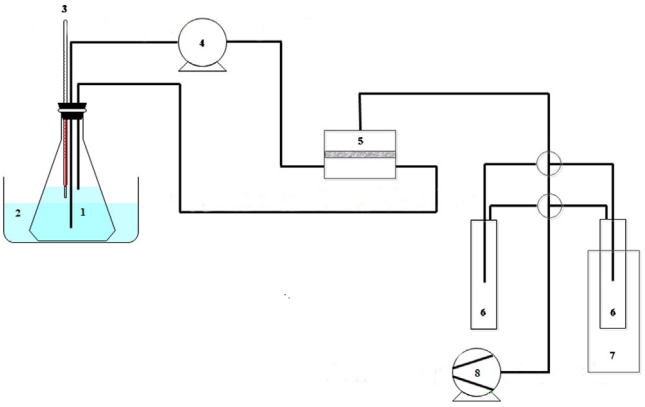

Fig. 1. Schematic diagram of PV unit (1) Feed container; (2) Water bath; (3) Thermometer; (4) Feed circulation pump; (5) Membrane permeation cell; (6) Permeate cold trap; (7) Liquid nitrogen container; (8) Vacuum pump.

an effective membrane area of 15.91 cm^2. The feed mixture was pumped from the feed tank (ca. 2 L) to the permeation cell through a centre opening and flowed radially along the membrane surface. To minimize the boundary layer effect, high feed circulation rate (3 L/min) was used. Vacuum was applied on the downstream side of the membrane using a vacuum pump. The permeate stream was condensed and collected in cold traps immersed in liquid nitrogen. The system was pre-operated for about 1h to attain steady state condition. After which, PV operation was performed for 2 h. The collected permeate sample was weighed and then analysed for composition using Agilent 7890A Gas Chromatography (GC) coupled with Agilent 220 Ion Trap Mass Spectrometer (MS). All reported values were averages of at least three experimental runs ($n = 3$).

From the obtained pervaporation experiment data, total permeation flux (J), separation factor (α), and pervaporation separation index (PSI) were calculated using the Eqs. (1)–(3):

$$J = \frac{W}{At} \tag{1}$$

$$\alpha_{sep} = \frac{P_o/P_w}{F_o/F_w} \tag{2}$$

$$PSI = J(\alpha_{sep} - 1) \tag{3}$$

where W is the mass of permeate (g); A, the effective membrane area (m^2); t, the permeation time (h); P_o and P_w are the mass percent of VFA and water in the permeate, respectively; F_o and F_w are the respective mass percent of VFA and water in the feed.

Results and discussion

Effect of different nanofiller loading

In order to select suitable nanofiller, three nanofillers graphene, graphene oxide and MoS_2 were dispersed in PEBA matrix. For convenience the PEBA–graphene, PEBA–graphene oxide and PEBA–molybdenum sulphide membranes were designated as PEBA/GP, PEBA/GO and PEBA/MS respectively. To compare the performance of the three membranes concentration of each filler was kept constant (0.25 wt%) for initial studies. The membranes were applied for PV separation using 6 g/L of butyric acid aqueous solution at 50 °C, since the butyric acid concentration in solutions produced by AD process was around 6 g/L. The obtained total flux and separation factor values are shown in Fig. 2. To compare the performance of composite membranes, PEBA membrane without any nanofillers was also applied for PV separation.

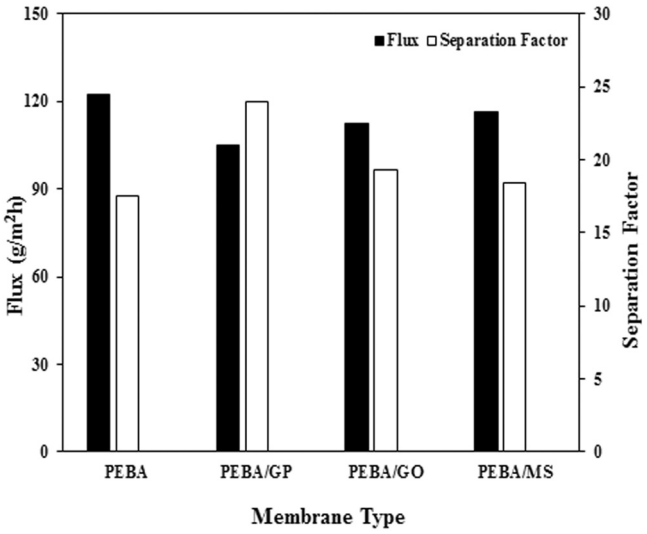

Fig. 2. Total flux and separation factor values of different composite membranes.

Addition of a nanofillers resulted in decrease of flux and slight increase in separation factor compared to pristine PEBA membrane. The decrease in the flux values is due to increase in the transport resistance as the fillers add resistance to the diffusion of molecules through the membrane. Higher separation factors of composite membrane might be due to increase in surface hydrophobicity of the membranes. In order to verify this surface hydrophobicity's of the membranes were analysed by estimating the water contact angles. The obtained results are shown in Fig. 3. Pure PEBA membrane showed contact angle 67 °, which is in good agreement with the reported value [34]. All the composite membranes showed higher contact angles than that of pure PEBA membrane and the contact angle values varied as PEBA/GP > PEBA/GO > PEBA/MS > PEBA, which is similar to the trend observed in the separation factor values. Therefore, this clearly supports the observation that the increase in separation factor for composite membranes is due to increase in the surface hydrophobicity. Compared to PEBA/GP membrane, PEBA/GO and PEBA/MS membranes showed lower contact angles, which might be due to the polar functional groups such as oxygen and sulphur on the graphene oxide and MoS_2 backbones. Among all the membranes PEBA/GP membrane showed the highest separation factor of 25 with the flux value of 104 g/m^2h.

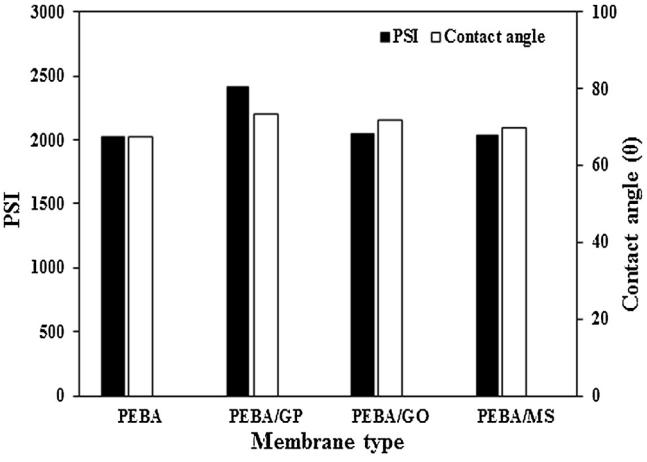

Fig. 3. PSI and contact angles of different composite membranes.

Pervaporation separation index (PSI) values were calculated using flux and separation factor values and the obtained values are shown in Fig. 3. PSI is the product of total flux and separation factor, which characterise the membrane separation ability. PSI can be used as a relative guideline for the selection of a membrane with an optimal combination of flux and separation factor. All the composite membranes showed higher PSI value than plane PEBA membrane and among the composite membranes PEBA/GP membrane showed highest PSI value which is due to highest separation factor exhibited by PEBA/GP membrane. Therefore, graphene was selected as nanofiller and PEBA/GP membranes were considered for further studies.

Effect of graphene loading

In order to see the effect of graphene loading on PV performance, PEBA-graphene membranes with different amount of graphene loading from 0.25 to 1 wt% were prepared. For brevity, these membranes were abbreviated as PEBA/GP-0.25, PEBA/GP-0.5, PEBA/GP-0.75 and PEBA/GP-1.0, respectively. Prior applying the membranes for PV separation, effect of graphene loading on physical properties of the membranes were analysed and the obtained results are discussed below.

Effect of graphene loading on membrane physical properties

Mechanical analysis. Incorporation of graphene in PEBA matrix enhanced the mechanical properties of PEBA to some extent. The obtained values of Young's modulus, ultimate tensile stress (UTS) and % strain at break are given in Table 1. The addition of graphene flakes increased the Young's modulus from 13 to 17 Mpa. PEBA/GP-0.75 showed Young's modulus of 17 MPa, an increase of 30% compared to pure PEBA membrane. Along with this graphene loaded membrane showed some improvement in the UTM values which increased from 22 MPa for pure PEBA membrane to 24 MPa for 0.75 wt% graphene loaded membrane. This is attributed to stronger interaction between graphene and PEBA polymer which offers resistance to the segmental movement of the polymer chains upon application of the tensile stress which leads to enhancement in modulus and ultimate tensile stress. On the other hand, the elongation at break of the composite membranes gradually decreased with increase in the graphene content which indicates that the ductility of the membranes has been decreased. This might be due to a large aspect ratio of graphene flakes and the interaction between graphene and the polymer matrix, which confines the movement of the polymer chains. Similar results were observed for other graphene-based polymer composites [35,36]. PEBA/GP-0.75 membrane showed highest mechanical properties and further increase in the graphene content (1 wt%) did not improve the mechanical properties. This could be due to restacking of graphene flakes after a critical filler loading level. This is typical behaviour observed in case of polymer nanocomposites, wherein beyond certain level of loading, tensile strength will not be significantly affected [37].

Differential scanning calorimetry (DSC). The heating scans of the DSC thermograms are shown in Fig. 4. The values of Tm and ΔHm of polyamide (PA) hard and polytrimethylglycol (PTMG) soft segments are tabulated in the Table 2. From Fig. 4 and Table 2, it is observed that the broad endothermic peak at around 9 °C is caused by the soft segment crystalline melting transition ($T_{m(ss)}$) of the PTMG phase of the PEBA matrix. The low temperature $T_{m(ss)}$ of PTMG segment is occurred because of its incapability to develop more regular ordered arrangement of the perfect lamellae crystals that is promoted in the PTMG homopolymer, which is also substantially restricted due to the presence of crystalline PA hard segment [38]. The high temperature small endothermic peak occurred at about 131 °C corresponds to the hard segment crystalline melting ($T_{m(hs)}$) peak of the PA phase of PEBA matrix. Both the $T_{m(ss)}$ and $T_{m(hs)}$ peak positions are slightly shifted to the higher temperature and also the enthalpies of melting ($\Delta H_{m(ss)}$) and ($\Delta H_{m(hs)}$) are increased with the graphene loading. It demonstrates that the crystallinity of the PEBA graphene composites is enhanced due to the positive nucleating effect in the presence of graphene [39]. This also indicates that there is a good interphase adhesion between the graphene and PEBA matrix. The glass transition temperature (T_g) associated with both the PTMG and PA were not observed in the present studies. It is mentioned in previous study [4] that due to broad thermal transitions it is difficult to precisely recognise T_g in case of PEBA polymer through DSC thermograms. This might be the reason why T_gs were not observed in the present study.

Thermogravimetric analysis (TGA). Thermal stability of the PEBA/GP membranes were examined using TGA under air atmosphere as

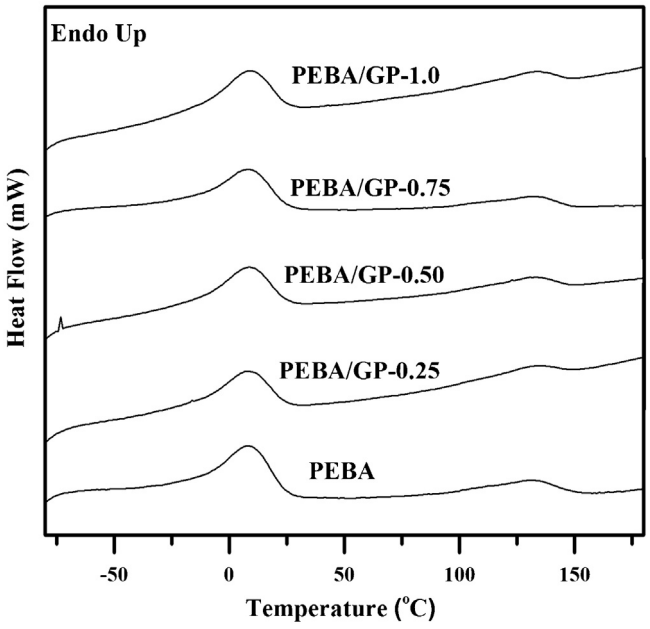

Fig. 4. DSC thermograms of PEBA and PEBA/GP composite membranes.

Table 1
Tensile properties of PEBA and PEBA/GP composite membranes.

Membrane	Young's modulus (Mpa)	UTS (Mpa)	% Strain at break
PEBA	13	22	1670
PEBA/GP-0.25	15	22	1564
PEBA/GP-0.5	16	23	1530
PEBA/GP-0.75	17	24	1481
PEBA/GP-1.0	17	22	1444

Table 2
DSC results of PEBA and PEBA/GP composite membranes.

Membrane	$T_{m(ss)}$ (°C)	$T_{m(hs)}$ (°C)	$\Delta H_{m(ss)}$ (J/g)	$\Delta H_{m(hs)}$ (J/g)
PEBA	7.7	130.7	32.2	8.1
PEBA/GP-0.25	8.2	131.1	32.1	8.3
PEBA/GP-0.5	8.7	131.0	35.5	9.7
PEBA/GP-0.75	8.8	132.4	34.9	11.0
PEBA/GP1.0	8.9	133.9	33.9	8.9

Please cite this article in press as: S.K. Choudhari, et al., J. Ind. Eng. Chem. (2014), http://dx.doi.org/10.1016/j.jiec.2014.08.010

shown in Fig. 5 and the results are summarized in Table 3. The thermograms show that the thermal stability of the PEBA polymer is increased by the incorporation of graphene. Especially the membrane with higher wt% of graphene loading showed significant improvement in the thermal stability. At 1 wt% graphene, the temperature at 10% and 50% weight loss are increased by 8 and 58 °C as compared to neat PEBA, respectively. These results show that the addition of graphene into the PEBA matrix at extremely low filling content could dramatically improve the thermal properties of the matrices. A similar increase in thermal stability has been reported in other polymer/graphene composites [40,41]. This substantial enhancement of thermal stability can be attributed to two reasons: first, the graphene platelets have high efficiency for capture of free radicals generated by polymer chain scission during the degradation process at high temperatures [42,43]. Secondly, the graphene platlets due to their high aspect ratio, acts as barrier and hinder the diffusion of volatile decomposition products in the PEBA matrix [44,45].

Effect of graphene loading on PV

To see the effect of graphene loading on PV performance, PEBA/GP membranes were applied for the PV separation of 6 g/L of aqueous butyric acid solution at 50 °C. The obtained flux and separation factor values are shown in Fig. 6.

With increase in the graphene loading total flux gradually decreased up to 0.75 wt% and then slightly increased for 1 wt% while separation factor showed an opposite trend, it increased up to 0.75 wt% and then decreased. To explain these results individual fluxes i.e. butyric acid flux and water flux values were calculated and plotted with respect to graphene loading (Fig. 7).

From the Fig. 7 it can be observed with increase in the graphene loading water flux is more affected compared to butyric acid flux. As graphene loading increased, water flux gradually decreased while butyric acid flux remained almost constant. When the graphene content in the membrane increases, the membrane surface hydrophobicity increases (shown in Fig. 8) which decreases water sorption leading to increase in the separation factor. On the other hand graphene platelets have a high aspect ratio and when the graphene content in the membrane increases, membrane transport resistance increases as the graphene platelets acts as barrier for the diffusing molecules through the membrane. Therefore, increase in separation factor and decrease in flux values at higher graphene loading is due to decrease in water flux values. However, PEBA/GP-1.0 membrane containing 1 wt% graphene loading showed slightly higher flux and decreased separation factor. This might be due to non-uniform dispersion of graphene flakes at higher wt% of graphene loading which might have generated voids in the membrane leading to faster diffusion of both butyric acid and water molecules and this led to increased flux and decreased separation factor. Similar observations were made by several other previous studies [32,46].

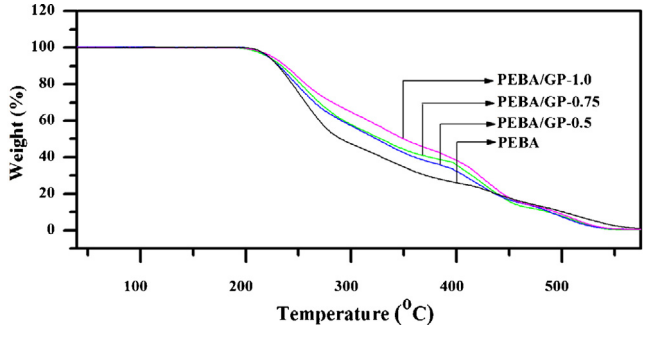

Fig. 5. TGA thermograms PEBA and PEBA/GP composite membranes.

Table 3
TGA data of PEBA and PEBA/GP composite membranes.

Membrane	T_{10} (°C)	T_{50} (°C)
PEBA	230.1	288.7
PEBA/GP-0.5	232.5	323.8
PEBA/GP-0.75	234.8	328.6
PEBA/GP-1.0	237.8	346.2

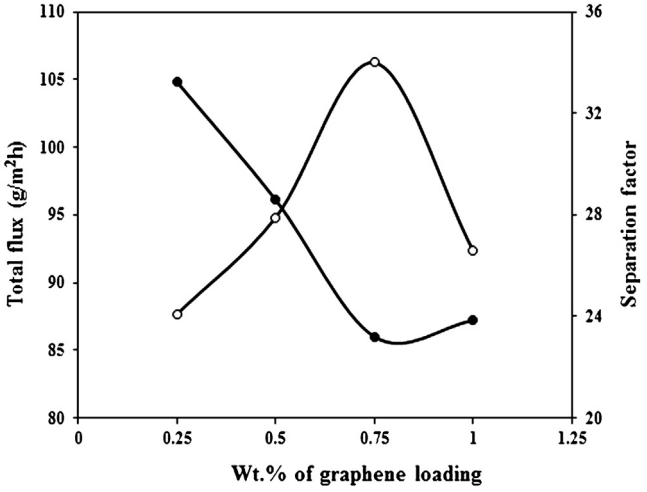

Fig. 6. Effect of graphene loading on total flux and separation factor.

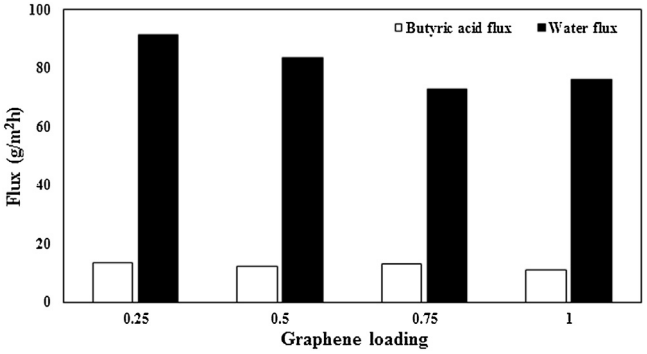

Fig. 7. Butyric acid flux and water flux values of different wt% graphene loaded membranes.

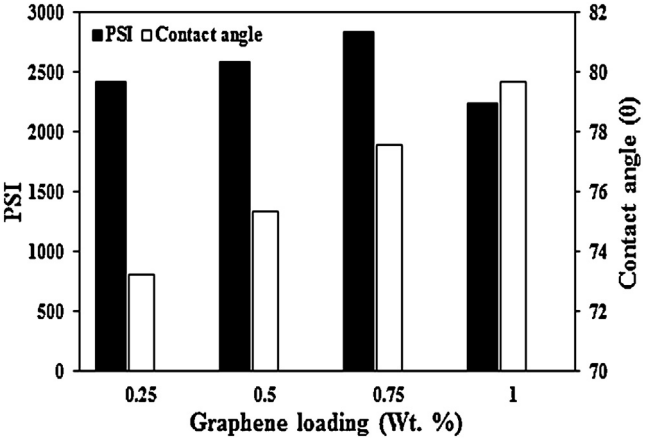

Fig. 8. Effect of graphene loading on PSI and contact angle.

Among the membranes PEBA/GP-0.75 membrane showed best performance with separation factor of 34 and permeation flux of 86 g/m^{2}h. PSI values of the membranes were estimated and are shown in Fig. 8. Expectedly, PEBA/GP-0.75 membrane showed highest PSI value which is due to high value of separation factor exhibited by the membrane and therefore, further studies continued with PEBA/GP-0.75 membrane.

Effect of temperature

To see the effect of operating temperature on PV, PEBA/GP-0.75 membrane was applied for PV separation of 6 g/L of butyric acid solution at different temperatures ranging from 40 to 70 °C and the observed flux and separation factors are shown in Fig. 9. As the feed temperature increased from 40 to 70 °C both the total flux and separation factor increased which is opposite to a normally observed trend wherein flux increases and separation factor decreases. In order to explain these results, individual fluxes i.e., butyric acid flux and water flux were estimated and plotted against operating temperature (Fig. 10).

From Fig. 10, it can be seen that increase in total flux and separation factor is due to increase in both the water and butyric acid fluxes. Increase in permeation flux is attributed to mainly two factors, one is increase of driving force across the membrane and other is increase in free volume of the membrane. As the temperature increases the vapour pressure on the feed side increases while on the permeate side remains unchanged due to which driving force across the membrane increases leading to increased mass transport. Along with this, the frequency and amplitude of the polymer chain jumping in the amorphous region increases at higher temperature which in turn increases the free volume in the membrane leading to higher permeation of molecules through the membrane. Both these factors increased the permeation flux. Increase in separation factor at higher temperature is attributed to increased permeation of butyric acid which might have resulted from the higher solubility of butyric acid at elevated temperatures. Butyric acid is an organic acid with a four carbon atoms and because of longer alkyl chain it exhibits hydrophobic nature and shows more affinity towards PEBA polymer. As the temperature increases solubility of butyric acid in the membrane increases leading to higher permeation of butyric acid which in turn increased the separation factor. Similar observations were made in several previous works [47,48].

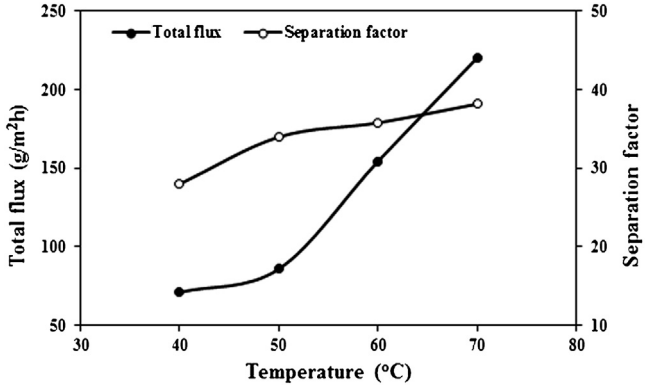

Fig. 9. Effect of temperature on PV performance.

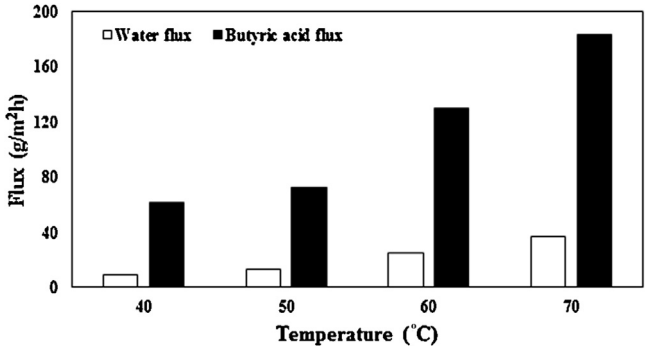

Fig. 10. Effect of temperature on butyric acid and water fluxes.

Effect of feed pH

In AD process, in order to lower the product inhibition effect, pH of the system is maintained between 5 and 7 at which acidogenic anaerobic microorganisms function well. Therefore, it is important to study the separation of carboxylic acid at relatively higher pH greater than pK_a value of the organic acids.

To study the effect of higher pH on pervaporation separation of butyric acid, PV experiments were carried out at 5.5 feed pH using PEBA/GP-0.75 membrane at 70 °C. Aqueous solution of butyric acid was prepared with concentration of 6 g/L and the solution showed pH of 3.8. The pH of the solution was re-adjusted to 5.5 by the addition of 2 N NaOH solution. The obtained values of total flux, water flux, butyric acid flux and separation factor are shown in Table 4.

When pH of the feed solution is increased it adversely affected butyric acid separation. Membrane yielded both lower flux as well as low separation factor at pH (5.5) compared to 3.8. This is due to decreased butyric acid flux. The pK_a value of butyric acid is 4.82 [49] and at a pH above this, butyric acid exists completely in the dissociated form. The solubility of butyric acid in water is more favoured in the dissociated state due to ionic interactions with water molecules. Therefore, this decreases the solubility of butyric acid in membrane leading to both lower separation factor and low flux value. Hence, this suggests that lower pH of the feed solution is more favourable for the pervaporation separation of butyric acid.

Effect of multicomponent feed mixture

In AD process along with butyric acid other acids such as acetic acid, propionic acid and valeric acid are also produced. Although, the quantity of butyric acid produced is high but other acids are also produced in a considerable amount. Therefore, it is important to study the effect of other acids in the feed mixture on butyric acid permeation and also the permeation behaviour of all the acids through membrane.

In order to understand the complex transport phenomenon of multicomponent feed mixture, a model solution mimicking the AD solution was prepared by dissolving acetic acid (0.5 g/L), propionic acid (0.25 g/L), butyric acid (6 g/L) and valeric acid (0.5 g/L) and applied for PV separation using PEBA/GP-0.75 membrane at 70 °C. Model solution showed 3.7 pH. Obtained fluxes and separation factor of all the acids are shown in Fig. 11.

Membrane showed total flux of 228.7 g/m^{2}h with water flux of 186.5 g/m^{2}h which are higher than the values obtained in case of

Table 4
Effect of feed pH on total flux, butyric acid flux, water flux and separation factor.

	pH 3.7	pH 5.5
Total flux	220.4	211
Butyric acid flux	37.1	27.3
Water flux	183.2	183.7
Separation factor	38.2	28

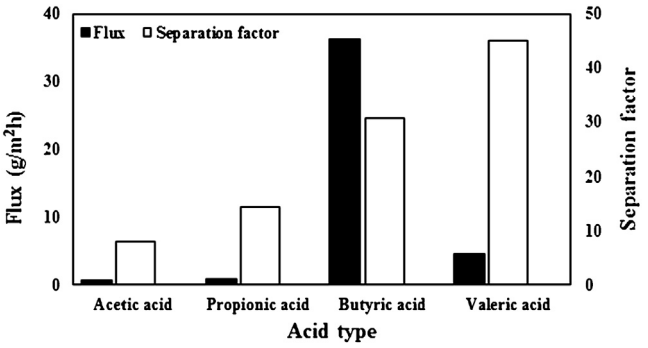

Fig. 11. Fluxes and separation factors of acetic, propionic, butyric and valeric acid obtained for model solution.

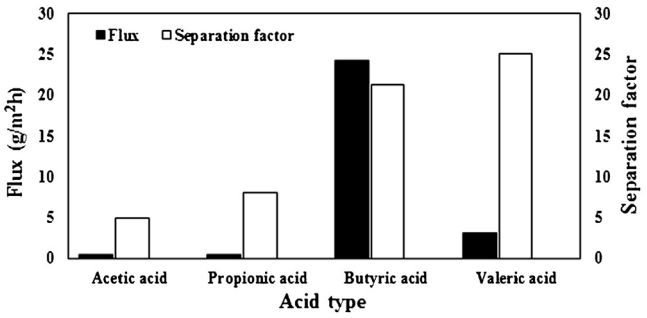

Fig. 12. Fluxes and separation factors of acetic, propionic, butyric and valeric acid obtained for AD solution.

binary feed mixture of butyric acid and water. This might be due to coupling effect. Organic acids especially acetic and propionic acid are highly soluble in water and can form strong hydrogen bonds with water molecules. These molecules might have dragged the water molecules with them while permeating through the membrane which resulted in both higher water flux and higher total flux. Among the four acids butyric acid showed the highest flux which is due to high concentration of butyric acid in the feed solution. Separation factor followed the trend as acetic acid - < propionic acid < butyric acid < valeric acid. This indicates that separation factor is mainly governed by the hydrophobicity of the acids. Hydrophobicity of the acids increases as the carbon chain length increases and due to which the hydrophobic interaction between permeant and membrane increases leading to higher sorption of the acid in the membrane resulting in a higher separation factor.

The butyric acid separation factor obtained for multicomponent mixture is lower than the separation factor obtained for binary mixture. This might be due to decreased permeant–membrane interaction in presence of permeant–permeant interactions. Acetic, propionic and valeric acids are polar molecules and can interact with butyric acid through dispersive, polar and hydrogen bonding interactions which decreases the interaction between butyric and membrane leading to decreased sorption of butyric acid in the membrane, finally resulting into reduced separation factor. Similar observation of decrease in the permeation of target component in presence of other components was made by several other researchers [50,51].

PV studies of AD solution from grass

AD solution obtained from the anaerobic digestion of perennial grass and dairy waste water was initially filtered through Whatman filter paper (No. 3) to remove the solid particles. Further the solution was ultrafiltered through Pelicon XL (Millipore) membrane system with membrane having 10,000 MWCO to remove the higher molecular weight impurities. The solution exhibited 5.7 pH and it is decreased to 3.7 by the addition of concentrated sulphuric acid. The concentrations of acetic acid, propionic acid, butyric and valeric acid in the solution were 0.52, 0.23, 5.95 and 0.60 g/L respectively. PV studies were carried out using PEBA/GP-0.75 membrane at 70 °C and the obtained results are shown in Fig. 12.

The fluxes and separation factors obtained for AD solution followed similar trend as in case of model multicomponent solution. However, the total flux as well as the individual fluxes and separation factors were lower than the model solution. This might be due to complex nature of AD solution. In AD process different kinds of micro-organisms work together to convert organic matter (carbohydrates, proteins and fats) into organic acids and molecular hydrogen. During the process several intermediates such as monosaccharides, amino acids and long chain fatty acids are generated and certain quantities of these unutilised intermediates may exists in the final AD solution along with VFAs. Along with this AD solution also contains several metal ions and colour impurities. All these components present in the AD solution might have hindered the permeation VFAs resulting in both reduced flux and separation factor. However, membrane showed good affinity for butyric acid, yielding flux of 24.3 g/m^{2}h with separation factor of 21. Comparing the concentration of butyric acid in feed (0.6%) with butyric acid in permeate (11.4%), indicates that the concentration has been increased almost 19 times and also the concentration of other acids in the permeate is very low (<2%). Therefore, this suggests that PEBA-graphene composite membrane can be used to concentrate butyric acid from AD solution through pervaporation technique.

Conclusion

PEBA based composite membranes were prepared and applied for the pervaporation separation of butyric acid. From the studies following conclusions were drawn.

1. PV membranes were prepared with three different 2D layered nanomaterials, graphene, graphene oxide and MoS_2 dispersed in PEBA matrix, graphene incorporated membrane showed the best performance which is attributed to higher hydrophobicity of the membrane exerted by the graphene platelets.
2. Increase in the graphene loading increased mechanical and thermal properties of the membranes and pervaporation studies showed PEBA membrane with 0.75 wt% graphene gives the best performance for the recovery of butyric acid among all the membranes, which is due to increased membrane hydrophobicity and transport resistance to water. Higher graphene loading beyond 0.75 wt% decreased membrane performance which is attributed to void formation due to agglomeration of graphene platelets.
3. Increase in the feed temperature increased both flux and separation factor which is attributed to increased driving force, increase in membrane free volume and higher dissolution of butyric acid in the membrane at elevated temperatures. Increase in the feed pH decreased the separation of butyric acid which is due to higher solubility of the butyric acid in water in the dissociated state.
4. Presence of other acid components in the feed solution decreased the permeation of butyric acid which is attributed to decreased permeant–membrane interaction in presence of permeant–permeant interactions.

Please cite this article in press as: S.K. Choudhari, et al., J. Ind. Eng. Chem. (2014), http://dx.doi.org/10.1016/j.jiec.2014.08.010

5. Pervaporation separation of AD solution showed lower separation performance than model multi component solution which is vowed to complex nature of AD solution.

This study demonstrates the use of novel nanocmposite membranes for PV process can offer cost-effective solutions for recovering the fine chemical produced by AD process.

Acknowledgements

This work was supported by the Technology Center for Biorefining and Bioenergy (Project no. CC20090004) www.tcbb.ie with the financial support of Enterprise Ireland and the Irish Industrial Development Agency (IDA).

References

[1] P.L. McCarty, Water Sci. Technol. 44 (2001) 149.
[2] A.E. Tugtas, Fen Bilimeri Dergisi 23 (2011) 7.
[3] J. Kuroiwa-Trzmielina, A. De Conti, C. Scolastici, D. Pereira, M.A. Horst, E. Purgatto, T.P. Ong, F.S. Moreno, Int. J. Cancer 124 (11) (2009) 2520.
[4] A. Rephaeli, R. Zhuk, A. Nudelman, Drug Dev. Res. 50 (3/4) (2000) 379.
[5] M. Bilgin, S.I. Kirbaslar, O. Oezcan, U. Dramur, J. Chem. Eng. Data 51 (5) (2006) 1546.
[6] J. Ebert, Biomass May. (2008) 29–32.
[7] D. Wu, H. Chen, L. Jiang, J. Cai, Z. Xu, P. Cen, Chin. J. Chem. Eng. 18 (4) (2010) 533.
[8] R.J. Zoetemeyer, A.J.C.M. Matthijsen, A. Cohen, C. Boelhouwer, Water Res. 16 (1982) 633.
[9] P.F. Pind, I. Angelidaki, B.K. Ahring, Biotechnol. Bioeng. 82 (2003) 791.
[10] Z. Wang, Y. Luo, P. Yu, J. Membr. Sci. 280 (2006) 134.
[11] C. Huang, T. Xu, Y. Zhang, Y. Xue, G. Chen, J. Membr. Sci. 288 (2007) 1.
[12] P. Gluszcz, T. Jamroz, B. Sencio, S. Ledakowicz, Bioprocess Biosyst. Eng. 26 (2004) 185.
[13] H.G. Joglekar, I. Rahman, S. Babu, B.D. Kulkarni, A. Joshi, Sep. Purif. Technol. 52 (2006) 1 (2006).
[14] N.A. Mostafa, Energy Convers. Manag. 40 (1999) 1543.
[15] M. Matsumoto, T. Otono, K. Kondo, Sep. Purif. Technol. 24 (2001) 337.
[16] A. Senol, U. Dramur, Solvent Extr. Ion Exch. 25 (2004) 865.
[17] M.M. Kabra, S.A. Netke, S.B. Sawant, J.B. Joshi, V.G. Pangarkar, Sep. Technol. 5 (1995) 259.
[18] A. Thongsukmak, K.K. Sirkar, J. Membr. Sci. 302 (2007) 45.
[19] M. Garcia, M.T. Sanz, S. Beltran, J. Chem. Technol. Biotechnol. 84 (12) (2009) 1873.
[20] J.C. Huang, M.M. Meagher, J. Membr. Sci. 192 (2001) 231.
[21] T. Ikegami, H. Yanagishita, D. Kitamotoa, H. Negishi, K. Haraya, T. Sano, Desalination 149 (2002) 49.
[22] T.C. Bowen, R.G. Meier, L.M. Vane, J. Membr. Sci. 298 (2007) 117.
[23] X. Tang, R. Wang, Z. Xiao, E. Shi, J. Yang, J. Appl. Polym. Sci. 105 (2007) 3132.
[24] S. Shi, Z. Du, H. Ye, C. Zhang, H. Li, Polymer 38 (2006) 949–955.
[25] H.W. Yen, S.F. Lin, I.K. Yang, J. Biosci. Bioeng. 113 (3) (2012) 372.
[26] B. Radisavljevic, A. Radenovic, J. Brivio, V. Giacometti, A. Kis, Nat. Nanotechnol. 6 (3) (2011) 147.
[27] J.E. Kim, T.H. Han, S.H. Lee, J.Y. Kim, C.W. Ahn, J.M. Yun, S.O. Kim, Angew. Chem. Int. Ed. 50 (13) (2011) 3043.
[28] G. Lalwani, A.T. Kwaczala, S. Kanakia, S.C. Patel, S. Judex, B. Sitharaman, Carbon 53 (2013) 90.
[29] J. Shen, Y. Zhu, X. Yang, C. Li, Chem. Commun. 48 (31) (2012) 3686.
[30] S. Mullick Chowdhury, G. Lalwani, K. Zhang, J.Y. Yang, K. Neville, B. Sitharaman, Biomaterials 34 (1) (2013) 283.
[31] R.R. Nair, H.A. Wu, P.N. Jayaram, I.V. Grigorieva, A.K. Geim, Science 335 (6067) (2012) 442.
[32] D.P. Suhas, A.V. Raghu, H.M. Jeong, T.M. Aminabhavi, RSC Adv. 3 (2013) 17120.
[33] F. Cerrone, S.K. Choudhari, R. Davis, D. Cysneiros, V. O'Flaherty, G. Duane, E. Casey, M.W. Guzik, S.T. Kenny, R.P. Babu, K. O'Connor, Appl. Microbiol. Biotechnol. 93 (2014) 611.
[34] L. Liu, Gas Separation by Poly(ether block amide) Membranes, University of Waterloo, Canada, 2008 p 55 (Chapter 3; Ph.D. thesis).
[35] Y. Xu, W. Hong, H. Bai, C. Li, G. Shi, Carbon 47 (2009) 3538.
[36] J.Y. Kong, M.C. Choi, G.Y. Kim, J.J. Park, M. Selvaraj, M. Han, Eur. Polym. J. 48 (2012) 1394.
[37] X. Zhao, Q. Zhang, D. Chen, Macromolecules 43 (2010) 2357.
[38] J.P. Sheth, J. Xu1, G.L. Wilkes, Polymer 44 (2003) 743.
[39] T. Kamal, S.Y. Park, M.C. Choi, Y.W. Chang, W.T. Chuang, U. Sereng, Polymer 53 (2012) 3360.
[40] B.J. Wang, Y.J. Zhang, J.Q. Zhang, Q. Gou, Z. Wang, P. Chen, Q. Gu, Chin. J. Polym. Sci. 31 (4) (2013) 670.
[41] I. Tantis, G.C. Psarras, D. Tasis, eXPRESS Polym. Lett. 6 (4) (2012) 283.
[42] S. Cheng, X. Chen, Y.G. Hsuan, C.Y. Li, Macromolecules 45 (2011) 993.
[43] S.L. Kodjie, L.Y. Li, B. Li, W.W. Cai, C.Y. Li, M. Keating, J. Macromol. Sci. Part B: Phys. 45 (2006) 231.
[44] M. Murariu, A.L. Dechief, L. Bonnaud, Y. Paint, A. Gallos, G. Fontaine, S. Bourbigot, P. Dubois, Polym. Degrad. Stab. 95 (2010) 889.
[45] T. Kuila, S. Bose, C.E. Hong, M.E. Uddin, P. Khanra, N.H. Kim, J.H. Lee, Carbon 49 (2011) 1033.
[46] S.K. Choudhari, M.Y. Kariduraganavar, J. Colloid Interface Sci. 338 (2009) 111.
[47] G.O. Yahaya, Sep. Sci. Technol. 44 (2009) 2894.
[48] N.L. Le, Y. Wang, T.S. Chung, J. Membr. Sci. 379 (2011) 174.
[49] J.A. Dean, Lange's Handbook of Chemistry, Fifteenth Edition, McGraw-Hill Inc, New York, N.Y., 1999.
[50] J. Huang, M.M. Meagher, J. Membr. Sci. 192 (2001) 231.
[51] S.Y. Li, R. Srivastava, R.S. Parnas, Biotechnol. Prog. 27 (1) (2011) 111.